A critical comparison of polypropylene and polyurethane sling materials after implantation in a suburethral sheep model

Anthony J. Bullock[a], David A. Gregory[a,b], Raouf Seyam[e], Falah Al-Mohanna[f], Omar Alsulaiman[e], Victoria L. Workman[a], Cornelia Rodenburg[a,b], Waleed Altaweel[e], Christopher R. Chapple[c,d], Sheila MacNeil[a,b]

[a]School of Chemical, Materials and Biological, Kroto Research Institute, University of Sheffield, Sheffield S3 7HQ, UK

[b]Insigneo Institute for in silico Medicine, University of Sheffield, Sheffield, UK

[c]Teaching Hospitals NHS Foundation Trust, Sheffield Children's NHS Foundation Trust and Doncaster and Bassetlaw Teaching Hospitals NHS Foundation Trust, Sheffield, UK

[d]Department of Urology, Sheffield Teaching Hospitals NHS Foundation Trust, Sheffield, UK

[e]Department of Urology, King Faisal Specialist Hospital and Research Center, Riyadh, Saudi Arabia

[f]Department of Comparative Medicine, King Faisal Specialist Hospital and Research Center, Riyadh, Saudi Arabia

Corresponding author:

Prof Sheila MacNeil, e-mail address: s.macneil@sheffield.ac.uk

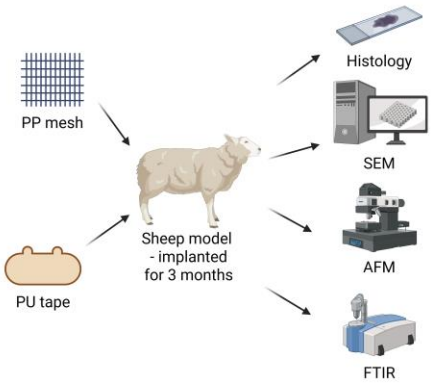

		PP mesh	PU tape
Histology	Tissue integration	Good	Good
	M1/M2 Inflammation	4.29	0.63
SEM	Surface degradation	Detected	Absent
AFM	Surface roughness	Increased	Slight increase
	Stiffness	Increased	Unchanged
FT-IR	Bulk composition	Degradation	Unchanged

Abstract

Although polypropylene (PP) materials have been implanted for decades for urethral support in the pelvic floor, appropriate large animal models and advanced materials analysis techniques have not previously been used to investigate the clinical problems they can cause - inflammation, pain and erosion through tissues

An ovine model duplicating the surgical procedure for suburethral sling surgery was developed. Here we present the results after 3 months implantation using immunohistochemistry and advanced materials characterisation of two materials PP and Polyurethane (PU).

Both materials were well integrated into the tissue. The M1/M2 ratio in PP-implanted tissue was statistically significantly elevated (4.29) compared to PU (0.63) and control tissue (0.34). The higher ratio indicates a more inflammatory response to PP than PU.

Surface roughness (assessed using atomic force microscopy) increased in both materials, Rq from 5.73-10.2nm in PP and from 1.03-2.96nm in PU; whilst Ra went from 4.75-7.85nm in PP and from 0.81-2.36nm in PU. Notably, surface stiffness increased by 0.05GPa in PP and decreased by 0.2GPa in PU. PP underwent both surface and bulk material degradation, PU did not.

Detailed testing of implantable materials in an appropriate animal model should be conducted before materials are introduced into clinical practice. It is salutary that this has never been reported before. The use of material characterisation techniques allowed us to identify problems in the performance of PP, notably surface degradation, changes in bulk properties and stiffening, which can activate macrophages. In contrast, PU appears a more suitable alternative material for use in treating patients with SUI.

Keywords: Stress urinary incontinence; Polypropylene; Polyurethane; Sheep model

1. Introduction

When polypropylene (PP) mesh was introduced for the treatment of stress urinary incontinence (SUI) and pelvic organ prolapse (POP) it was not assessed in any physiologically relevant animal model nor tested for its ability to support pelvic organs under intermittent strain. This study seeks to explore this research gap comparing the response of PP mesh to implantation in a physiologically relevant animal model comparing its response to that of a newer candidate material based on electrospun polyurethane (PU) which we have been developing as an alternative to PP-based materials.

The history of the use of PP in the pelvic floor arose from its prior use in abdominal hernia repair for over two decades. In those early applications, sustained inflammation and pain were reported in both animal studies and clinical cases where the material had been placed intra-abdominally. In response, manufacturers reduced the quantity of implanted material, which subsequently reduced the inflammatory burden and positioned it on a vascular layer of the abdominal wall to encourage tissue ingrowth. As a result, PP has been used with a relatively low complication rate in abdominal hernia repair for nearly 20 years [1].

However, the assumption that a material that is well tolerated in the abdominal cavity would perform similarly well in the pelvic floor has proved unfounded in a significant subset of patients when this was introduced [2]. At the time of its introduction for pelvic floor repair, no physiologically relevant animal models had been developed, and regulators did not require testing of this material for application in a new site in the body. For a comprehensive review of the

development and clinical introduction of mesh materials for the pelvic floor, please see Mangir et al. [2] and Roman et al. [3].

In brief, adverse clinical reports of PP mesh causing pain and contraction of mesh with erosion through the patients' tissues began to be reported [3]. Clinical adverse effects were most extreme where larger areas of mesh were used for POP repair, but even smaller strips of material used to provide support to the urethra led to pain and erosion in a significant proportion of patients. This culminated in the use of PP mesh being banned or restricted in its use in several countries including the UK.

At the time of writing several PP mesh manufacturers have been successfully sued by patients in the US, Australia and the UK. An unfortunate consequence of this is that despite the severity of the clinical problem there have been very few studies seeking to develop clinically acceptable alternatives to PP meshes to offer to women suffering from SUI and POP.

Accordingly, our long-term aim over the last 8 years has been to develop and evaluate a more acceptable alternative to PP mesh for use in treating the symptoms of SUI.

We hypothesised the problems encountered with the polypropylene meshes might be at least partially attributable to poor compliance matching between these strong but inflexible meshes and the site of implantation. Therefore, we developed a mesh designed to mimic the native connective tissue which has been used with considerable success to support the pelvic organs [3]. We selected a non-degradable polyurethane as the candidate material to replace polypropylene for several reasons; PUs proven ability to withstand repeated distension, its established use in other relevant FDA approved applications, its ability to be well tolerated post implantation and the fact that we could electrospin PU into a fascia-mimetic material. (Please see the discussion for

further details on the selection and characterisation of the PU used in this study).

Recognising that there has been little work in this area we have had several objectives over recent years - to develop and apply sensitive analyses of the surface properties of mesh to PP and PU mesh studied in vitro and following this to challenge these meshes with dynamic distension and oxidative stress [4,5]. We examined to what extent such challenged materials led to activation of cells to acquire a pro-contractile inflammatory and pro-scarring phenotype [6]. We then documented time dependent degradation of polypropylene surgical mesh explanted from the abdomen and vagina of sheep [7]. Our most recent objective was to develop a physiologically relevant animal model in which to explore materials to be inserted suburethrally for treatment of SUI. This model was published recently [8,9].

In this study we now use this sheep model to study materials implanted under the urethra to compare the effect of the PP and PU on the host response to these materials and to assess the impact of 3 months implantation on the physical properties of the two materials.

We applied an extensive combination of established histological and immunological techniques and physical methodologies to assess biological and physical changes in the materials after three months of implantation. Tissue integration and activation of immune cells were assessed by histology and immunohistochemistry and advanced surface analysis methods (SEM to examine surface integrity, AFM to assess surface roughness and mechanical properties and ATR-FTIR to assess bulk polymer stiffness [4-8,10-12]) were used to assess physical changes.

In summary, we report, for the first time, a critical comparison of this PU material and conventional PP mesh implanted under the urethra in a validated

large-animal model. By integrating immunohistochemical analyses with advanced surface characterisation, we provide evidence of early surface damage and stiffening of PP fibres after only three months.

2. Methodology

2.1 Description of sheep animal model and insertion of materials

All procedures were carried out following approval by the King Faisal Specialist Hospital and Research Center (Riyadh, Saudi Arabia) Institutional Research Board. The facility is accredited by the AAALAC (Association for Assessment and Accreditation of Laboratory Animal Care International). The hospital's Institutional Review Board (IRB) and the Animal Care and Use Committee reviewed and granted approval for the protocol (Ethics approval number: 2230017).

In this study, we sought to evaluate a trans-vaginal novel biomimetic material comprised of electrospun micro-fibers of polyurethane versus PP (TVT). The polyurethane implant has four holes for suture placement. Two lateral to allow approximation via suture up to the anterior abdominal wall and two holes to allow absorbable suture fixation to the periurethral fascial tissues deep to the vaginal mucosa to prevent the implant from sliding proximal to the urethra (Figure 1A and B).

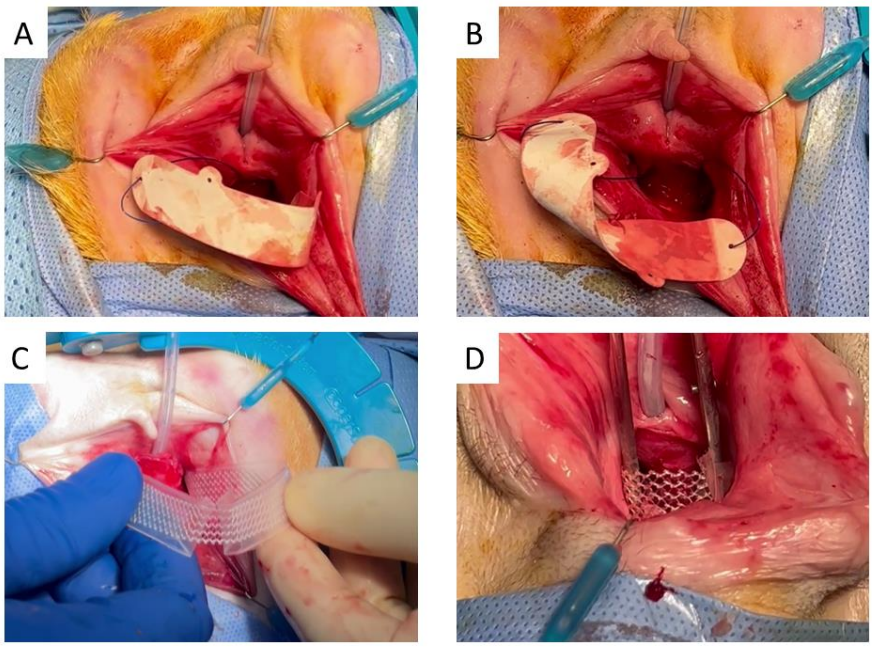

Figure 1. Surgical implantation of the PU device (A and B), and the PP device (C and D).

As reported in [8], 14 parous ewes with a median weight of 31.5 kg (SD 8.2) were included in this study. Under general anaesthetic, animals were placed in the lithotomy position. An incision was made on the ventral vaginal wall longitudinally. The tissue plane between the vaginal wall and the urethra was developed with lateral dissection using Metzenbaum scissors. Through the anterior vaginal wall incision, further dissection of the pelvic side wall was carried out on both sides allowing access into the retropubic space.

A 12-French Foley catheter was inserted. A standard transvaginal polypropylene tape (seven animals) or a fascia mimetic microfibre spun polyurethane tape (seven animals) were inserted using an introducer either via a suprapubic (seven animals) or a transvaginal approach (seven animals) into the suburethral and retropubic space (Figure 1). The incisions were closed, and the catheter was removed. A betadine vaginal pack was placed and removed after 24 hours. Postoperatively, the animals were observed carefully for pain and complications and allowed access to water and food under continuous veterinary supervision adhering to USA-approved protocols.

On the second postoperative day, all the animals passed urine freely and had regular bowel motions. No procedure related complications were observed.

2.2 Assessment of integration of materials into host tissue using histology and immunohistochemistry of explanted samples

The project #2230017 was approved for all the steps of the study including implantation, care of animals, harvest and euthanasia. Full details of the study till the endpoint were given in reference 25. After 3 months all animals were sacrificed as described previously. Samples of explanted tissues (from 7 sheep implanted with PU and 5 sheep implanted with PP, as two succumbed to pneumonia unrelated to the surgery or biomaterials) were placed in formalin (3.7% formaldehyde in PBS) and were dissected to provide a 1 cm x 2 cm block comprising the SUI implant and the surrounding tissue. Control samples were taken from tissue situated at least 3-4 cm away from the site of implantation. Samples (0.5 cm x 0.5 cm) were also snap frozen in liquid nitrogen. These two sets of samples were then couriered to the UK for histology, immunohistochemistry, and surface chemistry analysis.

The resulting blocks were embedded in wax and 6 μm sections taken. Multiple sections from each sample were taken to show a cross section of the urethras, the SUI device, and the tissue around the SUI device.

2.3 Tincture based histology

Sections from each of 12 samples were dewaxed in xylene and rehydrated by incubation in 100% ethanol, followed by incubation in 90%, 70% and 50% ethanol in dH_20. Slides were immediately stained with Haematoxylin and Eosin, Masson's Trichrome (Abcam, UK), or Van Gieson's stain (Abcam, UK), following each kit manufacturer's instructions. Stained slides were dehydrated in a series of alcohol solutions and mounted using DPX mountant (Sigma

Aldrich, UK). Bright field photographs were taken of each section under 40x magnification.

2.4 Immunohistochemistry

Slides were dewaxed as above then subjected to the antigen retrieval method advised by the antibody manufacturer. Samples were stained with rabbit recombinant monoclonal antibodies for smooth muscle actin (Abcam SP171, Abcam, UK), CD45 (Abcam EP322Y, Abcam, UK), and CD163 (Abcam EPR19518, Abcam, UK) and were incubated in Tris/EDTA buffer pH 9.0 at 95^{o}C for 20 minutes. Samples being stained with antibodies for CD43 (Abcam EP373Y, Abcam, UK) were incubated in citrate buffer pH 6 at 95^{o}C for 20 minutes. Samples were allowed to cool to room temperature before washing 3 times in PBS. Samples were then immunostained using a Rabbit Specific HRP/DAB Detection IHC Kit (Abcam ab64261, Abcam, UK) following the manufacturer's instructions. Antibodies were diluted as directed, Smooth muscle actin antibody was used at a dilution of 1:200, CD45 antibody at a dilution of 1:250, CD163 antibody at a dilution of 1:500, and CD34 antibody at a dilution of 1:2500. Samples were then dehydrated in a series of alcohol solutions and mounted using DPX mountant and bright field photographs were taken of each section under 40x magnification. Images were split to red, green and blue RGB channels using ImageJ (NIH, Maryland USA), the green channel images were thresholded (a value of 95 in ImageJ was used for all images) to isolate positive staining DAB staining and quantified.

2.5 Analysis of surface and bulk properties of explanted materials

2.5.1 Sample preparation

Prior to materials characterisation, the explanted mesh samples were thoroughly cleaned using a previously established procedure to remove any biological tissue adhering to the mesh surface [13]. Briefly, the cryo-frozen tissue samples containing mesh were treated with an alkaline solution (pH 8.5–9.5) containing

protease (Alcalase®, Merck, UK) at 37 °C for 72 hours. Alcalase® is a serine endopeptidase primarily composed of subtilisin A, which effectively hydrolyses proteins without damaging synthetic mesh materials. In other words, the cleaning process does not alter the mesh fibres. To validate the use of Alcalase® and provide a control, non-implanted polypropylene mesh (Restorelle from Coloplast - a mesh in common use until its recall by the FDA) was treated with the same Alcalase® solution used for the explanted materials.

2.5.2 (LV)-Scanning Electron Microscopy Imaging

The surface morphology of mesh samples (n = 3 for each material) were examined using a FEI Helios Nanolab G3 (FEI Company, US) microscope. Unlike conventional scanning electron microscopy (SEM) analysis, mesh samples were not coated with a conductive layer prior to imaging [5]. An accelerating voltage of 1–2 keV was applied under typical chamber vacuum pressures (approximately 10^{-6} mbar), with a working distance of 4 mm, to minimise surface charging and avoid sample damage. An Everhart-Thornley Detector (ETD) was used for low-magnification secondary electron (SE) imaging, and a Through Lens Detector (TLD) was used for high-magnification SE imaging.

2.5.3 Atomic Force Microscopy

Surface roughness of fibres and (Derjaguin–Muller–Toporov) DMT moduli were assessed using atomic force microscopy (AFM) in tapping mode using SCANASYST-AIR probes under ambient conditions with a Bruker Dimension Icon AFM. Mesh samples were placed on a cover glass and mounted on a magnetic AFM support. Multiple areas of each sample were analysed using PeakForce Tapping mode, which employs the maximum tip surface interaction force as a constant setpoint for each pixel scanned [14]. The tip was calibrated for absolute mechanical measurements using a Brucker calibration kit consisting of sapphire and titanium roughness standards to estimate the tip

dimensions and calibrate for Quantitative Mechanical Property Mapping (QNM mode). Data was processed using Bruker's NanoScope Analysis software (Version 2.0) and histogram frequencies were plotted as smoothed distribution curves for improved representation.

2.5.4 Assessment of the bulk properties of the polymers

Bulk properties were assessed using Attenuated Total Reflectance – Fourier-Transform Infrared Spectroscopy. Infrared spectra of the test mesh samples (n = 3 for each sample) were collected using a NICOLET 380 Fourier-transform infrared (FTIR) spectrometer (ThermoFisher Scientific, US) with an attenuated total reflectance (ATR) accessory fitted with a Golden Gate® diamond crystal (Specac). Spectra were recorded in the range of 500 to 4000 cm^{-1}, averaging 32 scans at a resolution of 4 cm^{-1}. All samples were analysed in solid-state form.

2.5.5 Statistics

Quantitative data obtained from immunohistochemistry images was subjected to two sample T tests, P values of < 0.05 were considered significant.

3. Results

All sheep were sacrificed at the end of 3 months. Tissue from 5 animals implanted with PP and 7 animals implanted with PU were excised and prepared for transport to the UK for analysis.

3.1 Assessment of integration of materials into the host animals by histological examination and immunohistochemistry of explanted samples

Hematoxylin and Eosin staining of Control tissues shows relatively compact collagen rich tissue (Figure 2A). Samples bearing an implant show that both the PP and PU implants show cell invasion and collagen deposition on the fibers of the implants (Figure 2B and C respectively). Tissue surrounding the PP implants in particular showed a higher degree of detachment from the surrounding tissue (Figure 2B) whereas the PU appeared to be in contact with surrounding tissue with observably less disruption (Figure 2C).

Masson's Trichrome staining confirms the collagen rich nature of the tissues (Figure 2D) indicated by blue staining. It also confirmed cellular invasion of both devices (red cytoplasmic staining) and collagen deposition (Figure 2E and F).

Van Gieson's staining showed the control samples to be rich in elastin (Figure 2G). The presence of PP (Figure 2H) and PU implants (Figure 2I) did not appear to alter the elastin content of surrounding tissue, but where disruption was present (Figure 2H) there was no elastin present in the collagen immediately adjacent to the implant.

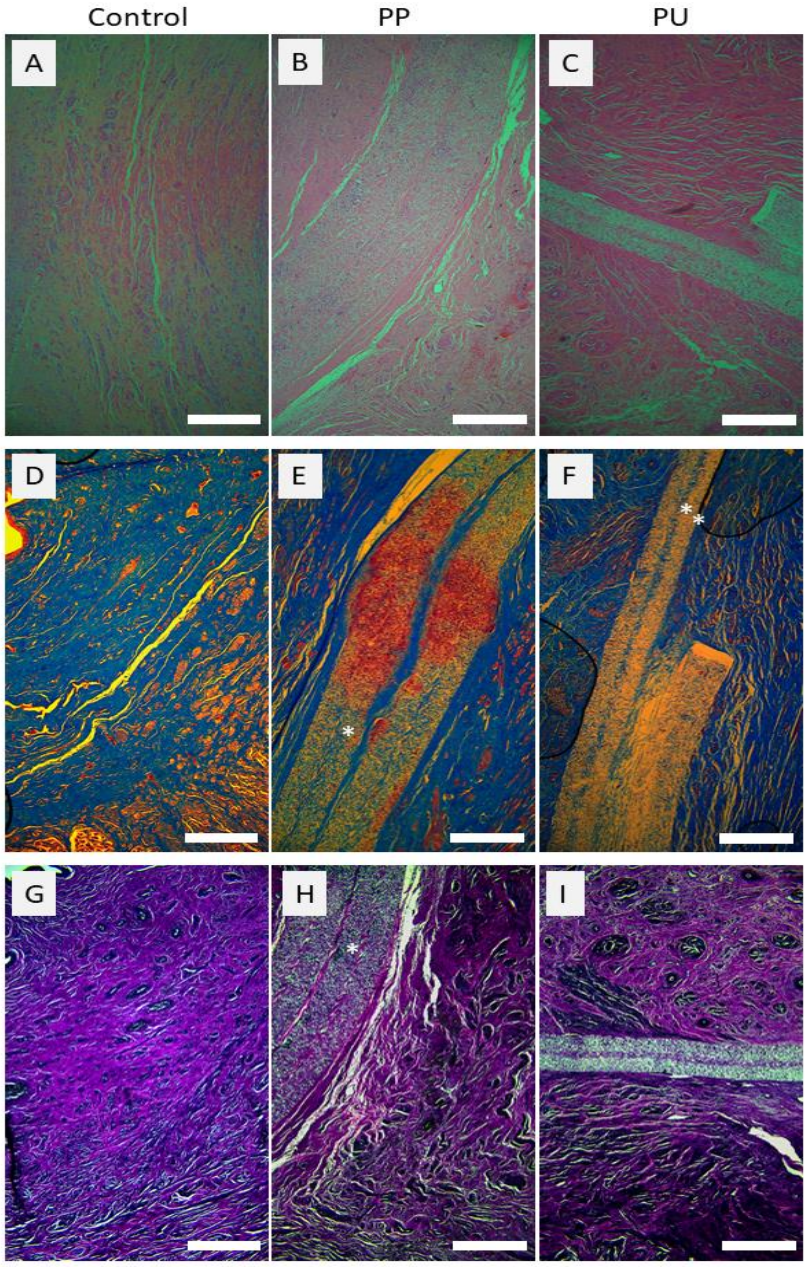

Figure 2. Histological staining of explanted tissue. Hematoxylin and Eosin staining of Control (A), PP implanted tissue (B) and PU implanted tissue (C). Masson's Trichrome staining of Control (D), PP implanted tissue (E) and PU implanted tissue (F) showing collagen staining (blue) and cytoplasm (red). Van Gieson's staining of Control (G), PP implanted tissue (H) and PU

implanted tissue (I) showing elastin (black) and collagen (purple). Devices are marked with *. Scale bar = 500µm.

The tissue of the urethra and surrounding tissue is rich in smooth muscle. Smooth muscle actin staining (Figure 3) shows Control (Figure 3A), PP implanted (Figure 3B), and PU implanted tissue (Figure 3C) to have similar smooth muscle content. This finding is confirmed in the numerical data summarised in Figure 7A where no statistical difference was seen although there are a small number of small pockets of SMA positive cells visible in samples taken from sheep implanted with both the PP and PU devices.

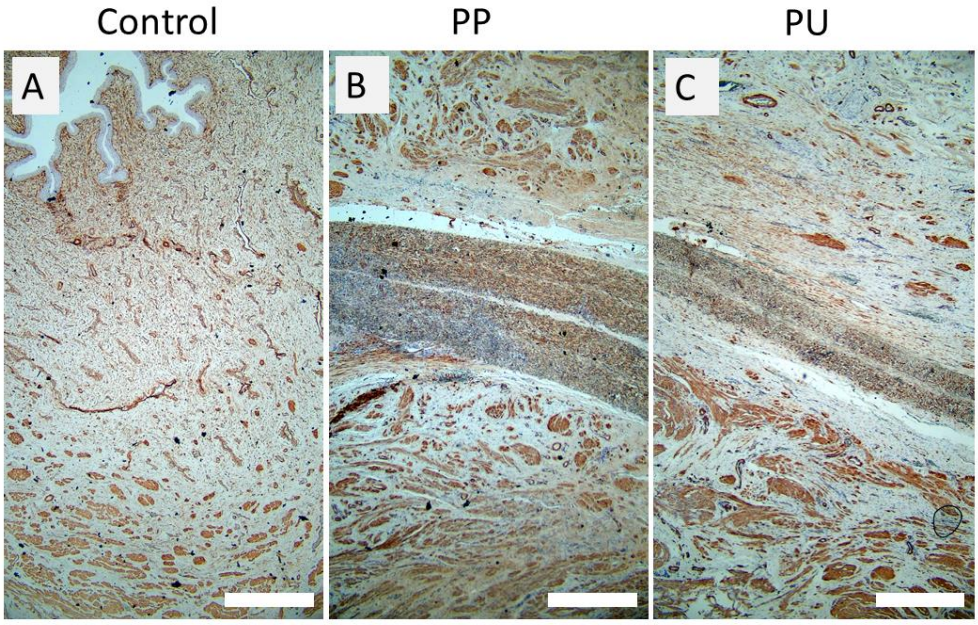

Figure 3. Representative images of immunohistochemical staining of smooth muscle actin in Control (A), PP implanted tissue (B) and PU implanted tissue (C). Dark brown DAB staining shows location of smooth muscle actin present in smooth muscle tissue. Scale bar = 500µm.

Immunohistochemical staining of CD34 in Control samples (Figure 4A) showed very few CD34 positive cells. Both PP and PU implanted tissue showed small pockets of CD34 positive cells (Figure 4B and C respectively), while PP implanted tissue appeared to have less CD34 staining than PU implanted tissue (Figure 7B) but neither were significantly different from control values.

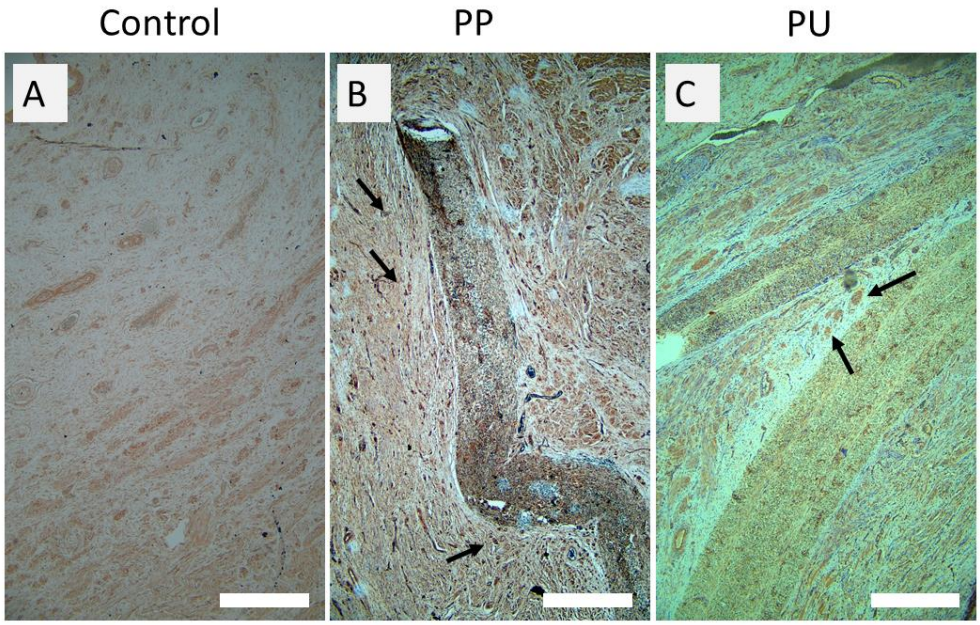

Figure 4. Representative images of immunohistochemical staining of CD34 Control (A), PP implanted tissue (B) and PU implanted tissue (C). Dark brown DAB staining shows location of CD34 positive cells, examples are marked with an arrow. Scale bar = 500µm.

Immunohistochemical staining of CD45 (Figure 5) and CD163 (Figure 6) was performed to assess the immunological reaction within the tissue to the implants. An M1 immune reaction is denoted by the presence of cells expressing CD45. Control tissues showed virtually no CD45 positive cells (Figure 5A) while both PP and PU implanted tissue showed observable pockets of CD45 positive cells (Figure 5B and C respectively). Staining was seen to be significantly increased compared to control in both implants, with PP implanted tissue showing CD45 staining significantly higher than PU implanted tissue (Figure 8A).

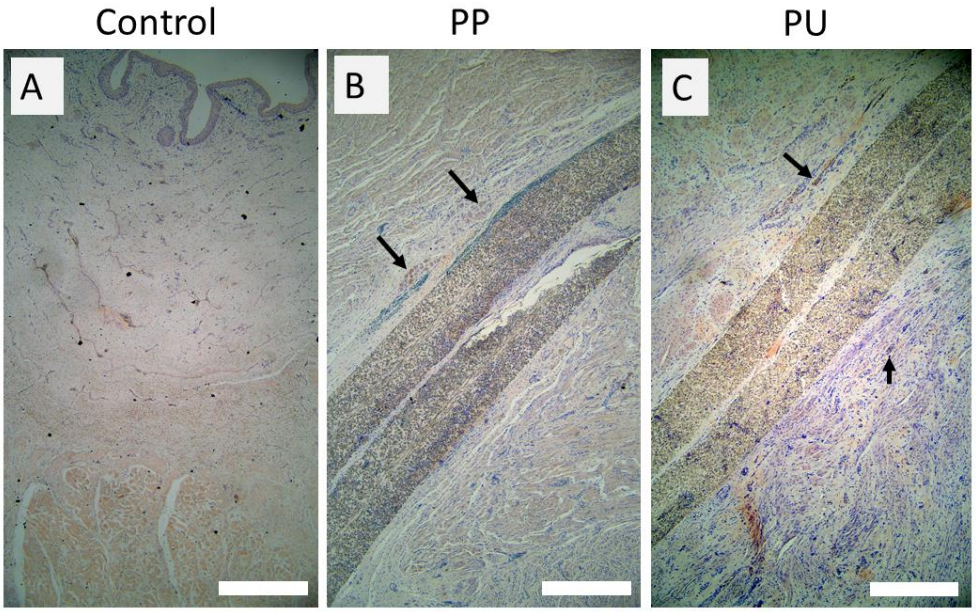

Figure 5. Representative images of immunohistochemical staining of CD45 Control (A), PP implanted tissue (B) and PU implanted tissue (C). Dark brown DAB staining shows location of CD45 positive cells exhibiting M1 immune reaction, examples are marked with an arrow. Scale bar = 500µm.

Expression of CD163 is associated with the M2 class of immune reaction. There was some degree of staining in all sections (Figure 6). This was least in control sections, more evident in tissue around PP, and strongest in tissue surrounding PU material. Staining was significantly higher in PU implanted tissue than control (Figure 8B).

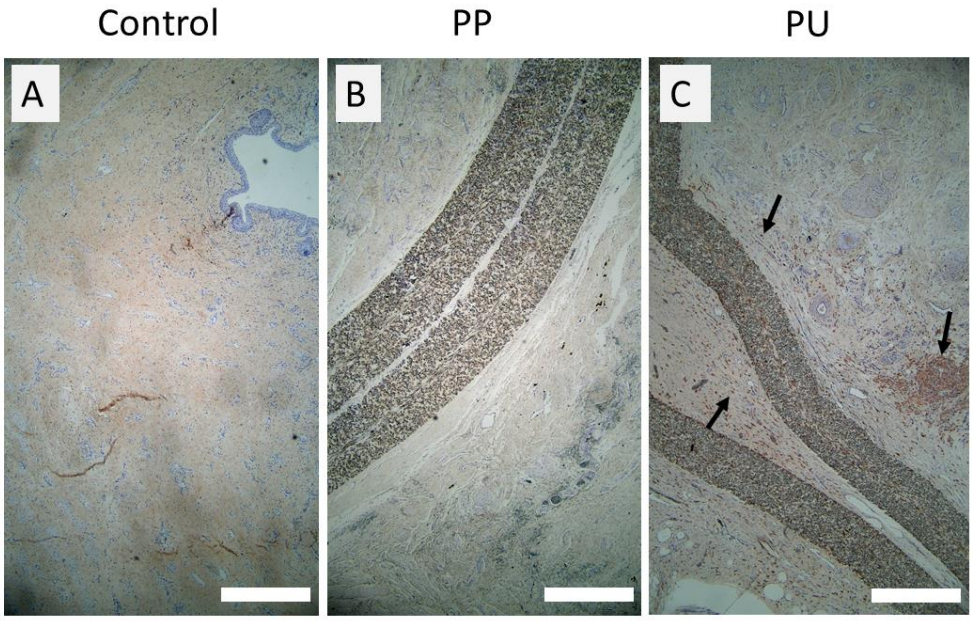

Figure 6. Representative images of immunohistochemical staining of CD163 staining in Control (A), PP implanted tissue (B) and PU implanted tissue (C). Dark brown DAB staining shows location of CD163 positive cells exhibiting M2 immune reaction, examples are marked with an arrow. Scale bar = 500µm.

The ratio of M1 / M2 immune expression calculated from the numerical CD45 and CD163 data obtained showed an M1/M2 ratio in control tissues of 0.34, 0.63 in PU implanted tissue and 4.29 in PP implanted tissues.

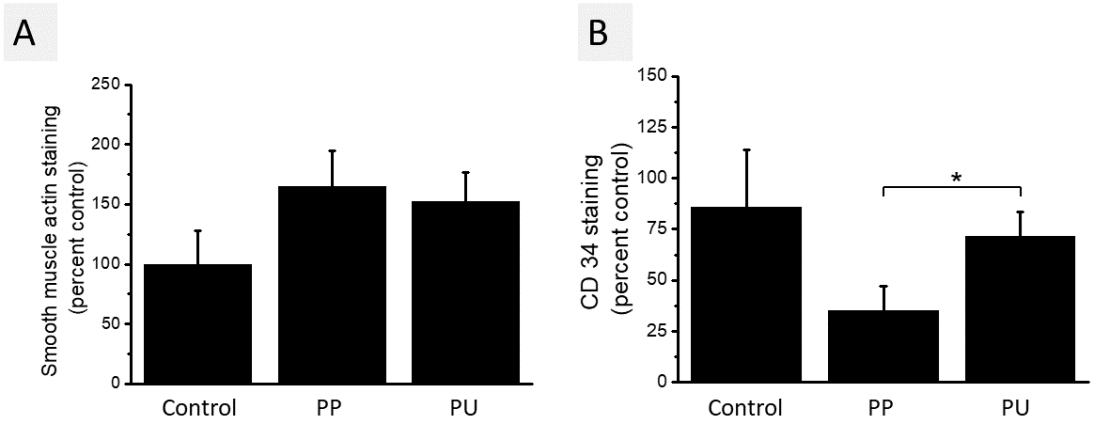

Figure 7. (A) Comparison of smooth muscle actin staining in Control (n=4), PP implanted tissue (n=5) and PU implanted tissue (n=9). (B) Comparison of CD34 staining in staining in Control (n=4), TVT implanted tissue (n=5) and PU implanted tissue (n=7). Data was obtained from immunohistochemical staining, statistical significance was determined by two sample T-test, and $P<0.05$ was deemed significant.

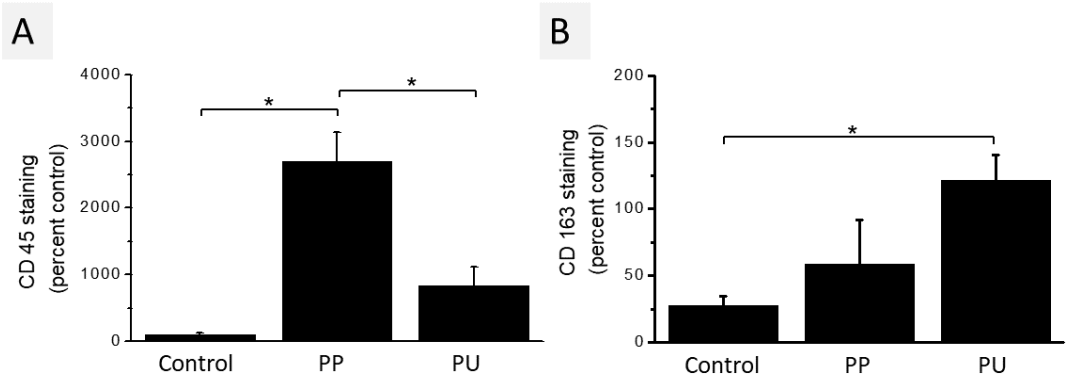

Figure 8. (A) Comparison of CD45 staining in Control (n=4), PP implanted tissue (n=5) and PU implanted tissue (n=9) indicating cells exhibiting M1 immune reaction. (B) Comparison of staining in Control (n=4), PP implanted tissue (n=4) and PU implanted tissue (n=6) indicating cells exhibiting M2 immune reaction. Data was obtained from immunohistochemical staining,

statistical significance was determined by two sample T-test, and $P<0.05$ was deemed significant.

3.2 Summary of integration of materials into host tissues

Histological examination shows that both devices are invaded by cells and support collagen deposition with some small evidence of elastin deposition within both devices. There is also evidence for smooth muscle actin expression within both devices, suggesting that fibroblasts within the device are encountering a degree of mechanical distension. Revascularization shown by CD34 expression is also suggested by the positive staining in the region of the devices, though this was not a strong response in these samples. Both devices elicited an immune response in the tissue surrounding the implant, but there was a clear difference in the nature of that response, as PU elicited a strong M2 response with an M1/M2 ratio similar to that of control tissue while PP elicited an M1 response significantly greater than both control and PU giving a high ratio of M1 to M2 indicative of a strong inflammatory response.

3.3 Analysis of surface of explanted materials

Low-voltage scanning electron microscopy (LV-SEM) images of explanted PP and PU meshes are shown in Figure 9A and 9B, respectively. Inset images depict the control materials prior to implantation. In the case of PP (Figure 9A), there is clear evidence of surface degradation following explantation. While a longitudinal pattern is visible in both the control and explanted samples, likely originating from the fibre extrusion process, additional features such as transverse cracking/markings and the presence of surface particulates are observed only in the explanted samples. These observations suggest that the PP fibres underwent degradation in vivo.

In contrast, the PU fibres (Figure 9B) appear unchanged following explantation. No visible cracks or particulates are apparent, and the fibres remain comparable in appearance to those of the control sample. This indicates that the PU mesh

has greater morphological stability than the PP during the 3-month implantation period.

Surface roughness was assessed with three-dimensional atomic force microscopy (AFM). Height maps of PP and PU mesh are shown in Figure 9C and D. Both figures include images from the control and explanted samples. A marked increase in surface roughness is evident for both materials after explantation. For the PP samples, the root mean square roughness (Rq) increased from 5.73 nm in the control to 10.2 nm in the explanted sample, while the average roughness (Ra) increased from 4.75 nm to 7.85 nm. Similarly, for the PU samples, Rq increased from 1.03 nm to 2.96 nm and Ra from 0.81 nm to 2.36 nm.

These changes in roughness suggest that surface modifications occurred during the 3 months of implantation. In the case of PP, this is in agreement with the LV-SEM data and further supports a model of surface degradation through mechanical or oxidative processes. For PU, although LV-SEM did not reveal visible surface defects, the increase in roughness suggests the presence of more subtle surface nanoscale alterations.

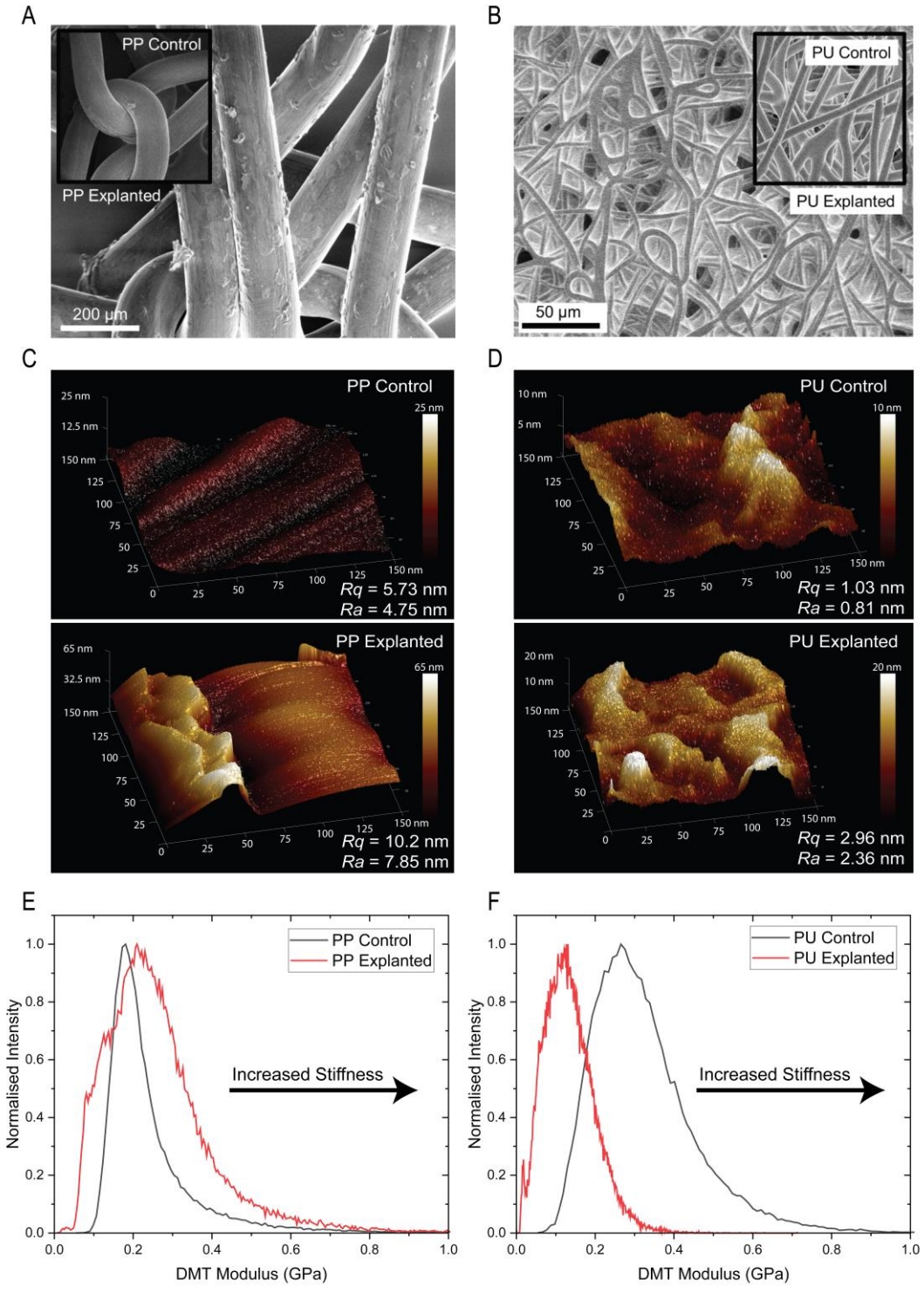

Figure 9. Morphological, topographical, and mechanical characterisation of explanted polypropylene (PP; A, C, E) and polyurethane (PU; B, D, F) meshes. (A, B) Low-voltage SEM images show pronounced surface degradation in explanted PP fibres. (C, D) AFM height maps reveal increased surface roughness in both PP and PU after explantation. (E, F) Derjaguin–Muller–Toporov (DMT) modulus histograms indicate increased stiffness in explanted PP.

3.4 Analysis of stiffness of materials

Distribution curves of Derjaguin–Müller–Toporov (DMT) modulus values are presented in Figure 9E for PP and 9F for PU. For PP, the explanted sample exhibits a noticeable shift in the modulus distribution, with the peak moving approximately 0.05 GPa higher than that of the control.

This increase in stiffness is consistent with previous studies, which have shown that mechanical distension of polypropylene meshes can result in surface stiffening [7]. Such in vivo stiffening is clinically relevant, as it can lead to complications due to mismatches between the mechanical properties of the implant and surrounding tissues. These mismatches may contribute to issues such as chronic pain or mesh erosion.

For PU, the opposite trend is observed. The modulus distribution curve for the explanted sample shows a reduction in stiffness, with a peak approximately 0.2 GPa lower than that of the control. This softening of the material may result from degradation mechanisms known to affect polyurethane in physiological environments [15]. One possibility is chemical degradation through hydrolytic or oxidative processes. Exposure to water, enzymes, and reactive oxygen species, particularly from inflammatory cells such as macrophages, can result in chain scission, lowering molecular weight and disrupting crosslinking, which in turn reduces stiffness. An alternative or additional mechanism may involve plasticisation, whereby absorbed water, lipids, or proteins from surrounding tissue increase chain mobility. This increased mobility reduces the effective stiffness of the material and is consistent with the observed decrease in modulus.

3.5 Analysis of bulk properties of polymers

Attenuated Total Reflectance – Fourier-transform infrared (ATR-FTIR) spectroscopy was used to investigate chemical changes in the PU and PP meshes before and after implantation (Figure 10). The spectra for the PU control and explanted samples were very similar, indicating that the bulk chemical structure of the material remained stable during the implantation period. Characteristic absorption bands associated with polyurethane were observed in both spectra, including a strong peak between 1725 and 1740 cm^{-1} corresponding to carbonyl (C=O) stretching of urethane groups, and a shoulder near 1725 cm^{-1} consistent with hydrogen-bonded carbonyl species. Additional features between 1600 and 1530 cm^{-1}, attributed to the amide II band involving N–H bending and C–N stretching, and bands in the 1300 to 1000 cm^{-1} range consistent with C–N and C–O stretching, were also retained. The absence of new peaks or significant spectral shifts suggests that any degradation of the PU material was confined to the surface and not detectable by ATR-FTIR, which probes the bulk composition. This interpretation is supported by the observed decrease in stiffness and increase in surface roughness, implying that while the surface of the PU mesh may have undergone some degree of plasticisation or early-stage degradation, the overall chemical structure remained intact.

Spectra taken outside of the fingerprint region showed no peaks for isocyanate groups in the PU material either before or after implantation - please see SI for details of this.

In contrast, the ATR-FTIR spectra for the PP control and explanted samples revealed clear differences. Both spectra retained the characteristic bands of polypropylene, such as CH_2 and CH_3 bending vibrations between 1450 and 1375 cm^{-1}, and features between 1200 and 1000 cm^{-1} due to C–C stretching and CH wagging modes. However, the explanted PP sample exhibited additional absorptions not present in the control. A distinct peak at approximately 1740

cm^{-1} and a shoulder around 1725 cm^{-1} were identified, features that are not associated with pristine polypropylene. These signals are indicative of carbonyl-containing degradation products, such as carboxylic acids, and are commonly observed in cases of oxidative degradation.

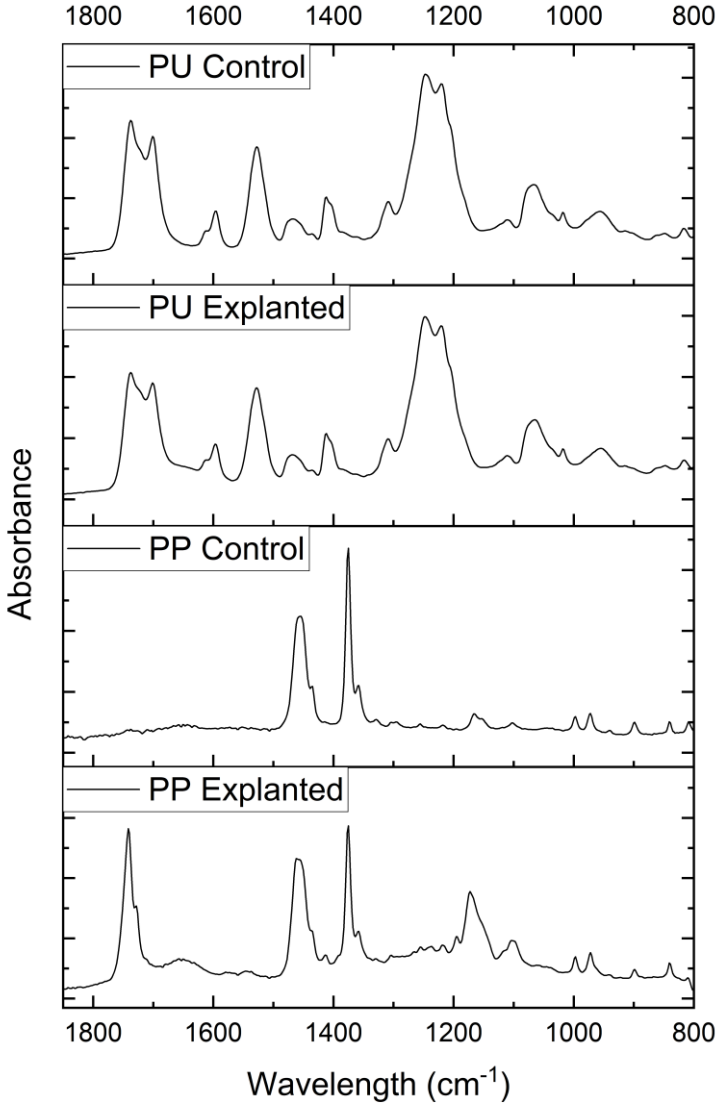

Figure 10. FTIR Spectra of control and explanted mesh samples.

Our ATR-FTIR analysis of the PP samples revealed the presence of carbonyl groups (~1700–1750 cm^{-1}), indicating surface oxidation induced by cellular activity. Polypropylene has been shown to undergo oxidative modification in response to reactive oxygen species (ROS) generated by cells during

metabolism or inflammatory responses as shown in Farr et al. [5, 6]. The interaction of PP with ROS is further described in the discussion section below.

4. Discussion

The aim of this study was to undertake a critical evaluation of the tissue response and material performance of a PU device compared to a commercially available PP implant using a large physiologically relevant animal model.

4.1 Prior animal work

Although some early animal work was undertaken, including a study conducted approximately 11 years after the introduction of the tension-free PP vaginal tape (TVT) procedure [16, 17], these focused largely on mechanical fixation and lacked detailed histological evaluation. The first study to clearly demonstrate that PP mesh behaves differently depending on the site of implantation came from Jan De Prest's group in 2017 [18]. Using a sheep model for POP repair, they compared PP mesh implanted into the abdomen versus mesh implanted in the rectovaginal space [18]. While abdominally placed mesh retained over 90% of its area over six months, the same mesh implanted in the rectovaginal space contracted by 50%, with extrusion of mesh through the vagina occurring in 3 out of 10 animals.

We suggest physiologically relevant animal models are essential for testing biomaterials intended for pelvic floor applications as insertion of materials into the abdomen of animals has not identified the problems which are encountered when mesh materials are used to support the urethra in women.

Additional insights have come from macaque models, which provided critical evidence that anatomical site and mesh orientation influence host response [19-27]. More recently, Isali et al. described a sheep model using bottom-up tape insertion in three ewes, similar in approach to the model used in the present study, though their work lacked detailed histological analysis [28].

As a key step in developing and evaluating new materials for use in SUI we reported the development of a sheep model for under-urethra implantation of both PP mesh (using a TVT device) and a novel PU material [8]. The model accommodates both retrograde (bottom-up) and top-down approaches, and a companion video article provides a detailed procedural overview [9].

4.2 Selection of polyurethane for development as an alternative material to PP

Polyurethanes have emerged as versatile and promising biomaterials owing to their exceptional biocompatibility, mechanical strength, and the ability to be tailored for specific applications - as reviewed in [29]. They have demonstrated significant potential across various medical domains from tissue engineering and wound healing to cardiovascular devices and bone repair.

Polyurethanes have been used since the 1940s, primarily in construction industries where their versatility and ability to withstand compression have made them one of the largest classes of polymers in use [30, 31]. They are synthetic copolymers containing urethane linkages linking three monomers: a diisocyanate, a polyol and a chain extender. This enables the synthesis of a large number of polyurethanes with different physicochemical and mechanical properties. The physicochemical properties are largely dependent on the conformation of polyols, which may contain two or more different polyols, stabilisers, catalysts, liquids or solid additives and, in the case of foams, foaming agents. Depending on the structure of the polyols, i.e. the length of the chain, structure of the units (aliphatic or aromatic), ester or ether groups, or functionalisation by hydroxyl groups, polyurethanes may be flexible or rigid, and therefore suitable for various applications.

A key feature of these polymers is their ability to sustain contractile forces. This feature has led to them being used in a wide range of non-medical applications such as phones and upholstery and more recently in biomedical applications where they have found applications, primarily because of their ability to sustain

contractile forces without undergoing any deterioration in the polymer structure or capability. Of most relevance to the current application, they have found applications in cardiac devices where they cope with the forces that originate during the cardiac cycle without undergoing plastic deformation or failure. Other applications of PUs in this field include biostable implants and cardiovascular implantable devices such as cardiac pacemakers, catheters, prostheses, cardiac assist devices, heart patches, heart valves, stents and vascular grafts [29].

We selected this PU (PU Bionate) purchased from DSM Biomedical B.V, The Netherlands, because it was already in clinical use and approved by the FDA for use in several applications. As stated in the DSM product information file "Bionate® PCU is an industry-leading medical grade polymer for use in long-term implants. It has been used in chronically implanted medical devices for nearly two decades. The Bionate® PCU family is currently being used in a wide range of applications, including neurostimulation, vascular, artificial heart, cardiac assist and diagnostic devices."

We fabricated the PU to mimic native connective tissue by electrospinning 3 layers of material - 2 layers of random microfibres with a central layer of parallel nanofibres [32]. This material withstands repeated cyclic distension in contrast to several PP materials which demonstrated irreversible distension under the same conditions [3].

For FDA-commissioned reports summarising the clinical response to both PP and PU, see fda.gov/media/152350 and fda.gov/media/152352, respectively.

4.3 Prior investigations into the suitability of PP and PU as materials to treat SUI

We evaluated PU in comparison with PP both for mechanical properties and for biocompatibility in a series of animal experiments where the immune response

to the material was assessed post-implantation in rat abdomen for 7 days [33], in rabbit abdomen for 3 months [32] and in sheep vagina for 6 months [28]. In the current study, we have gone beyond previous work by using a physiologically relevant animal model (implantation under the urethra of sheep) and carried out extensive testing of the physical properties of the two materials. We also assessed the impact of these materials on adjacent tissue following three months of implantation in the sheep model. The in-depth materials analyses were all informed by our prior studies on PP degradation [4-6], including the first characterisation of titanium-coated PP mesh in humans [11], and the most comprehensive analysis to date on the in vivo degradation of PP [7].

4.4 Comparative results on implanting PP and PU for 3 months in sheep model

In this study both materials were implanted sub-urethrally in a position equivalent to that used clinically in mid-urethral sling procedures. Tissue and materials were harvested after three months to assess biological and mechanical outcomes through histological, immunohistochemical, and material analyses.

Surgical implantation was successful with no adverse effects observed in the sheep throughout the implantation period. Histological examination confirmed that both implant types were well integrated into host tissues, supporting cellular infiltration, collagen deposition, and new blood vessel formation, consistent with successful tissue incorporation. CD34 expression, indicative of vascularisation, was evident around both implants, although not significantly elevated, suggesting some degree of revascularisation. Van Gieson staining indicated preservation of elastin content in most samples; however, localised regions surrounding the PP mesh showed reduced elastin deposition, implying tissue disruption and matrix remodelling.

Immune profiling revealed distinct responses to the two materials. Macrophage staining showed both M1 (pro-inflammatory) and M2 (wound

healing/remodelling) phenotypes present in tissues adjacent to implants. Notably, the M1/M2 ratio in PP-implanted tissue was statistically significantly elevated (4.29) compared to PU (0.63) and control tissue (0.34), indicating that PP induces a sustained pro-inflammatory environment. In contrast, PU elicited a predominantly M2-dominant immune profile, consistent with constructive tissue remodelling. Smooth muscle actin (SMA) staining demonstrated that smooth muscle content in the surrounding urethral tissue was retained across all groups, with SMA-positive cells present within implant regions, possibly reflecting mechanical loading or cellular differentiation, warranting further investigation. The proposed mechanism for PP leading to inflammation and pain in women begins with cellular production of reactive oxygen species (ROS). During normal metabolism or immune responses, cells generate reactive species. These ROS can interact with the PP polymer chains, removing hydrogen atoms from the tertiary carbons in the backbone and thereby forming macroradicals on the PP surface. The macroradicals can subsequently react with oxygen, generating peroxy radicals that decompose to form carbonyl-containing species such as ketones, aldehydes, and carboxylic acids, which are detectable by ATR-FTIR. This cell-induced oxidation modifies the surface chemistry of PP, introducing polar functional groups that can influence cell adhesion, wettability, and overall biocompatibility as discussed in [5, 6].

Material analyses further differentiated the two materials. As these materials were implanted using a novel clinically relevant animal model and subsequently processed in a different manner compared to previous studies, direct comparison with earlier explanted PP mesh studies is not possible. However, the results showed similar degradation trends [7, 11]. LV-SEM revealed surface cracking and particulates on PP fibres, consistent with oxidative degradation in vivo. PU fibres showed no obvious surface defects on LV-SEM; however, AFM detected an increase in nanoscale surface roughness after implantation (from 8

nm to 20 nm), which may reflect early-stage hydrolytic or oxidative alterations or biofouling rather than overt degradation. AFM measurements also showed PP fibres to have higher initial surface roughness (25 nm), which increased substantially (to 65 nm) post-implantation.

AFM mechanical testing demonstrated that PP fibres stiffened after implantation, likely due to mechanical distension and polymer chain crosslinking associated with oxidative degradation. Such increased stiffness can lead to mismatches between implant and host tissue mechanical properties, which have clinical implications including pain and erosion [10]. Conversely, PU fibres exhibited a slight decrease in stiffness, potentially due to surface-level degradation or plasticisation effects from biomolecule absorption, resulting in increased polymer chain mobility.

ATR-FTIR spectroscopy supported these observations. PP showed minor spectral changes indicative of chemical degradation and oxidation of polymer bonds, whereas PU exhibited no significant bulk compositional changes after implantation, suggesting that any degradation processes were surface-localised and minimal.

Together, these findings demonstrate that the combination of a clinically relevant large animal model and sensitive analytical techniques can effectively detect significant differences in the biological response and material integrity of candidate implants for stress urinary incontinence. PP mesh, despite its widespread clinical use, induces a persistent inflammatory environment, undergoes surface degradation, and stiffens post-implantation, factors that likely contribute to adverse outcomes such as pain and tissue erosion observed clinically. In contrast, PU mesh shows a more favourable immune profile, maintains structural integrity with only subtle surface changes, and exhibits mechanical compliance more aligned with native tissues. This suggests PU may

offer a more biocompatible and durable alternative for mid-urethral sling procedures, designed to accommodate extensive and irregular mechanical distension over long durations.

4.5 Clinical translation

We propose that this study potentially translates into the clinical application of this material leading to less risks to the patient in a number of ways. Firstly, we have conducted an exhaustive comparison of the body's response to polypropylene and polyurethane (based on three months implantation under the sheep urethra), and in particular we have looked critically at how this implantation under the urethra actually affects the physical properties of the materials.

When PP meshes were introduced into the pelvic floor for pelvic organ prolapse and for SUI it was without any rigorous follow-up or testing in any relevant animal model which are reported in the literature. One consequence of the last more than fifteen years of patients' suffering a range of adverse complications when PP meshes are used is that many patients have lost confidence in their surgeons and the manufacturers of polypropylene mesh products. Recognising this, it is imperative that the introduction of any new material needs rigorous preclinical investigation to avoid any predictable adverse tissue reactions to an implanted biomaterial.

Recent studies compiling the problems encountered by patients receiving PP mesh for SUI report pain in up to 52% of patients, erosion of the mesh materials through the patients' tissues in 4% of patients, sexual dysfunction in 2.4 % of patients and a reoperation rate of up to 12% [34-37]. With these potentially impactful complications on quality of life when PP mesh is used in some patients it is clearly essential that we develop a better material that does not cause these adverse responses.

In this report we have developed a physiologically relevant animal model relevant to the clinical procedure which allows precise preclinical evaluation of tissue reactivity to the insertion of any material under the urethra. This has allowed a critical appraisal of the performance of PU versus PP in this model.

PU outperforms PP in causing a milder inflammatory response (hence one would expect less pain) and little evidence of any change in physical properties - whereas PP clearly became more rigid with clear signs of surface damage. It was possible to demonstrate these changes in just 3 months post implantation

in this sheep model. We conclude that initial testing of new materials versus existing PP materials using this animal model and range of tests allows one to critically discriminate between existing PP materials likely to cause problems and new materials, such as electrospun PU, which (in contrast to PP) mimics the ability of native fascia to cope with the repeated and irregular distension seen upon implantation in the dynamic environment of the pelvic floor.

However, the real challenge of introducing any new material for use as a permanent implant in an area where patients have experienced an unacceptable level of complications cannot be ignored.

4.6 Future research directions

To progress this work towards the clinic we suggest the next steps would be to submit this data to the FDA for their review requesting approval to conduct a first in woman safety study. Here we will look critically at the effects of the new material on urinary continence and look for any evidence of pain developing. We would propose that results of continence and pain be reported after 1, 2 and 5 years of implantation to reassure women that the PU material can offer long term relief from the symptoms of SUI without the threat of biomaterials related complications.

5. Conclusion

We report, for the first time, that implantation of SUI candidate materials for just three months in a physiologically relevant large-animal model can reveal subtle adverse changes in the surface and bulk properties of PP. In contrast, PU remained largely unchanged and was well tolerated.

Conventional immunohistochemistry showed that both materials were well tolerated in terms of tissue ingrowth, collagen deposition, and smooth muscle content. However, their immune responses differed. In adjacent tissues, macrophages exhibited an M1/M2 expression ratio of 0.34 in controls, 0.63 in PU-implanted tissues, and 4.29 in PP-implanted tissues. The higher ratio observed with PP indicates a markedly more inflammatory response compared to PU. Sustained inflammation is a well-recognised complication associated with PP.

Advanced microscopy techniques were employed to quantify material properties. As we have previously demonstrated, LV-SEM is invaluable for detecting surface degradation linked to macrophage activation [6], and here it confirmed surface damage in PP but not in PU fibers. AFM revealed an increase in surface stiffness of PP fibers, whereas PU fibers remained unchanged. ATR-FTIR analysis further demonstrated alterations in the bulk chemical structure of PP consistent with oxidation, while PU showed no detectable changes.

PU was selected as an alternative to PP for urethral support due to its flexibility, resilience to repeated distension, and long history of use in FDA-approved devices. Since PP complications are often associated with post-implantation stiffening, a material that maintains its mechanical stability may be more suitable for this application. Taken together, these findings from a physiologically relevant large-animal model suggest that PU carries a lower risk

of patient complications compared to PP and provide a strong preclinical evidence base for progressing to first-in-women studies, pending FDA approval.

Funding

We would like to acknowledge the Urology Department, King Faisal Specialist Hospital and Research Centre, and the Robert Luff Foundation for unrestricted education grants for funding the animal experiments samples and funding the histology and immunohistochemistry of explanted tissues. The work on physical characterisation of materials was supported by Engineering and Physical Sciences Research Council (EPSRC) EP/V012126/1.

Acknowledgments

We would like to thank the Sorby Centre for Electron Microscopy at the University of Sheffield for allowing electron microscopy and analysis to be performed. We acknowledge the use of the Henry Royce Nanocharacterisation Laboratory at The University of Sheffield. The graphical abstract was created using Biorender.

Declaration of competing interest

The authors have not received funding from commercial organisations for the development of this work over the last eight years. The University of Sheffield and Sheffield Teaching Hospitals hold a joint patent (WO2018/224836A1) on the development of the polyurethane electrospun material, which was filed on 13th December 2018.

Data statement

The data that support the findings of this study are available from the corresponding author, (SMN), upon reasonable request.

References

[1] Fadaee, N., Huynh, D., Khanmohammed, Z., Mazer, L., Capati, I., Towfigh, S, Patients with systemic reaction to their hernia mesh: an introduction to mesh implant illness, J. Abdom. Wall Surg. 2 (2023) p.10983. doi: 10.3389/jaws.2023.10983.

[2] Mangir, N., Aldemir Dikici, B., Chapple, C.R., MacNeil, S, Landmarks in vaginal mesh development: polypropylene mesh for treatment of SUI and POP, Nat. Rev. Urol. 16 (2019) 675-689. doi: 10.1038/s41585-019-0230-2.

[3] Roman, S., Mangir, N., Hympanova, L., Chapple, C.R., Deprest, J., MacNeil, S, Use of a simple in vitro fatigue test to assess materials used in the surgical treatment of stress urinary incontinence and pelvic organ prolapse, Neurourol. Urodyn. 38 (2019) 107-115. doi: 10.1002/nau.23823.

[4] Farr, N.T., Roman, S., Schäfer, J., Quade, A., Lester, D., Hearnden, V., MacNeil, S., Rodenburg, C, A novel characterisation approach to reveal the mechano–chemical effects of oxidation and dynamic distension on polypropylene surgical mesh, RSC Adv. 11 (2021) 34710-34723. doi: 10.1039/D1RA05944K.

[5] Farr, N.T., Rauert, C., Knight, A.J., Tartakovskii, A.I., Thomas, K.V, Characterization and quantification of oxidative stress induced particle debris from polypropylene surgical mesh, Nano Sel. 4 (2023) 395-407. doi: 10.1002/nano.202200243.

[6] Farr, N.T., Workman, V.L., Saad, S., Roman, S., Hearnden, V., Chapple, C.R., Murdoch, C., Rodenburg, C., MacNeil, S, Uncovering the relationship

between macrophages and polypropylene surgical mesh, Biomater. Adv. 159 (2024) 213800. doi: 10.1016/j.bioadv.2024.213800.

[7] Farr, N.T.H., Gregory, D.A., Workman, V.L., Rauert, C., Roman, S., Knight, A.J., Bullock, A.J., Tartakovskii, A.I., Thomas, K.V., Chapple, C.R., Deprest, J., MacNeil, S., Rodenburg, C, Evidence of time dependent degradation of polypropylene surgical mesh explanted from the abdomen and vagina of sheep, J. Mech. Behav. Biomed. Mater. 160 (2024) 106722. doi: 10.1016/j.jmbbm.2024.106722.

[8] Chapple, C.R., Seyam, R., Alsulaiman, O., Bullock, A.J., Al-Mohana, F., MacNeil, S., Altaweel, W, Development of a clinically relevant preclinical animal model to mimic suburethral implantation of support materials for stress urinary incontinence, Neurourol. Urodyn. 44 (2025) 489-495. doi: 10.1002/nau.25630.

[9] Seyam, R., Chapple, C., Alsulaiman, O., Al-Mohanna, F., MacNeil, S., Altaweel, W. A Novel Surgical Technique in a Sheep Model for Suburethral Graft Implantation. J. Vis. Exp.: JoVE, 220 (2025) e67282. doi:10.3791/67282.

[10] Farr, N.T, Regulating the formation and extent of crazing through the application of argon plasma surface functionalisation, Polym. Test. 128 (2023) 108244. doi: 10.1016/j.polymertesting.2023.108244.

[11] Farr, N.T., Klosterhalfen, B., Noé, G.K, Characterization in respect to degradation of titanium-coated polypropylene surgical mesh explanted from humans, J. Biomed. Mater. Res. B: Appl. Biomater. 111 (2023) 1142-1152. doi: 10.1002/jbm.b.35221.

[12] Farr, N.T., Workman, V.L., Chapple, C.R., MacNeil, S., Rodenburg, C, Strengthening preclinical testing to increase safety in surgical mesh, Nat. Rev. Urol. 21 (2024) 515-516. doi: 10.1038/s41585-024-00889-5.

[13] Wang, H., Klosterhalfen, B., Müllen, A., Otto, T., Dievernich, A., Jockenhövel, S, Degradation resistance of PVDF mesh in vivo in comparison to PP mesh, J. Mech. Behav. Biomed. Mater. 119 (2021) 104490. doi: 10.1016/j.jmbbm.2021.104490.

[14] Fakhrullina, G., Akhatova, F., Kibardina, M., Fokin, D., Fakhrullin, R, Nanoscale imaging and characterization of Caenorhabditis elegans epicuticle using atomic force microscopy, Nanomedicine: nanotechnology, biology, and medicine. 13 (2017) 483–491. doi: 10.1016/j.nano.2016.10.003.

[15] Vakil, A. U., Petryk, N. M., Du, C., Howes, B., Stinfort, D., Serinelli, S., Gitto, L., Ramezani, M., Beaman, H. T., Monroe, M. B. B., In vitro and in vivo degradation correlations for polyurethane foams with tunable degradation rates. J Biomed Mater Res A, 111(2023) 580–595. doi: 10.1002/jbm.a.37504.

[16] Ulmsten, U., Henriksson, L., Johnson, P., Varhos, G, An ambulatory surgical procedure under local anesthesia for treatment of female urinary incontinence, Int. Urogynecology J. 7 (1996) 81-86. doi: 10.1007/BF01902378.

[17] Rezapour, M., Novara, G., Meier, P.A., Holste, J., Landgrebe, S., Artibani, W, A 3-month preclinical trial to assess the performance of a new TVT-like mesh (TVTx) in a sheep model, Int. Urogynecology J. 18 (2007) 183-187. doi: 10.1007/s00192-006-0130-x.

[18] Urbankova, I., Callewaert, G., Sindhwani, N., Turri, A., Hympanova, L., Feola, A., Deprest, J, Transvaginal mesh insertion in the ovine model, J. Vis. Exp.: JoVE. 125 (2017) 55706. doi: 10.3791/55706.

[19] Artsen, A.M., Rytel, M., Liang, R., King, G.E., Meyn, L., Abramowitch, S.D. and Moalli, P.A, Mesh induced fibrosis: the protective role of T regulatory cells, Acta Biomater. 96 (2019) 203-210. doi: 10.1016/j.actbio.2019.07.031.

[20] Artsen, A.M., Mayr, C.A., Weber, K., Rytel, K., Moalli, P.A, Polypropylene surgical mesh induces lipid oxidation in a nonhuman primate model, Acta Biomater. 198 (2025) 207-218. doi: 10.1016/j.actbio.2025.04.003.

[21] Barone, W.R., Knight, K.M., Moalli, P.A., Abramowitch, S.D, Deformation of transvaginal mesh in response to multiaxial loading, J. Biomech. Eng. 141 (2019) 021001. doi: 10.1115/1.4041743.

[22] Brown, B.N., Mani, D., Nolfi, A.L., Liang, R., Abramowitch, S.D., Moalli, P.A, Characterization of the host inflammatory response following implantation of prolapse mesh in rhesus macaque, Am. J. Obstet. Gynecol. 213 (2015) 668-e1. doi: 10.1016/j.ajog.2015.08.002.

[23] Knight, K.M., King, G.E., Palcsey, S.L., Suda, A., Liang, R., Moalli, P.A, Mesh deformation: A mechanism underlying polypropylene prolapse mesh complications in vivo, Acta Biomater. 148 (2022) 323-335. doi: 10.1016/j.actbio.2022.05.051.

[24] Liang, R., Abramowitch, S., Knight, K., Palcsey, S., Nolfi, A., Feola, A., Stein, S., Moalli, P.A, Vaginal degeneration following implantation of synthetic mesh with increased stiffness, BJOG: Int. J. Obstet. Gynaecol. 120 (2013) 233-243. doi: 10.1111/1471-0528.12085.

[25] Nolfi, A.L., Brown, B.N., Liang, R., Palcsey, S.L., Bonidie, M.J., Abramowitch, S.D., Moalli, P.A, Host response to synthetic mesh in women with mesh complications, Am. J. Obstet. Gynecol. 215 (2016) 206-e1. doi: 10.1016/j.ajog.2016.04.008.

[26] Shaffer, R.M., Liang, R., Knight, K., Carter-Brooks, C.M., Abramowitch, S., Moalli, P.A, Impact of polypropylene prolapse mesh on vaginal smooth muscle in rhesus macaque, Am. J. Obstet. Gynecol. 221 (2019) 330-e1. doi: 10.1016/j.ajog.2019.05.008.

[27] Therriault, M.A., Kottapalli, S., Artsen, A., Knight, K., King, G., Meyn, L., Brown, B.N., Moalli, P.A, Profiling of the macrophage response to polypropylene mesh burden in vivo, Biomaterials. 318 (2025) 123177. doi: 10.1016/j.biomaterials.2025.123177.

[28] Isali, I., Khalifa, A.O., Shankar, S., Dannemiller, S., Horne, W., Evancho-Chapman, M., McClellan, P., MacLennan, G.T., Akkus, O., Hijaz, A, Comparison of morphological and histological characteristics of human and sheep: sheep as a potential model for testing midurethral slings in vivo, Urol. Int. 107 (2023) 422-428. doi: 10.1159/000522138.

[29] Cui, M., Chai, Z., Lu, Y., Zhu, J., Chen, J, Developments of polyurethane in biomedical applications: A review, Resour. Chem. Mater. 2 (2023) 262-276. doi: 10.1016/j.recm.2023.07.004.

[30] Pivec, T., Smole, M.S., Gašparič, P., Kleinschek, K.S., Polyurethanes for Medical Use, Tekstilec. 60 (2017) 182-197. doi: 10.14502/Tekstilec2017.60.182-197.

[31] Joseph, J., Patel, R.M., Wenham, A., Smith, J.R., Biomedical applications of polyurethane materials and coatings, Transactions of the IMF, 96 (2018) 121–129. doi: 10.1080/00202967.2018.1450209.

[32] Roman, S., Urbánková, I., Callewaert, G., Lesage, F., Hillary, C., Osman, N.I., Chapple, C.R., Deprest, J., MacNeil, S, Evaluating alternative materials for the treatment of stress urinary incontinence and pelvic organ prolapse: a comparison of the in vivo response to meshes implanted in rabbits, J. Urol. 196 (2016) 261-269. doi: 10.1016/j.juro.2016.02.067.

[33] Przydacz, M., Adli, O.E.Y., Mahfouz, W., Loutochin, O., Bégin, L.R., Corcos, J, Structural differences and architectural features of two different polypropylene slings (TVT-O and I-STOP) have no impact on biocompatibility

and tissue reactions, Cent. Eur. J. Urol. 70 (2017) 154-162. doi: 10.5173/ceju.2017.1189.

[34] Badri, H., Rajai, A., Ward, K., Edmondson, R., & Reid, F. The management of vaginal prolapse and stress incontinence mesh complications in a quaternary mesh complications service in the United Kingdom (U.K): a 5-year observational study. BMC women's health, 25 (2025) 381. doi: 10.1186/s12905-025-03916-8.

[35] Jha, S., Ammenbal, M., & Metwally, M. Impact of incontinence surgery on sexual function: a systematic review and meta-analysis. The journal of sexual medicine, 9 (2012) 34–43. doi: 10.1111/j.1743-6109.2011.02366.x.

[36] Muller, P., Gurol-Urganci, I., van der Meulen, J., Thakar, R., & Jha, S. Risk of reoperation 10 years after surgical treatment for stress urinary incontinence: a national population-based cohort study. American journal of obstetrics and gynecology, 225 (2021) 645.e1–645.e14. doi: 10.1016/j.ajog.2021.08.059.

[37] Moore, R. D., & Lukban, J. C. Comparison of vaginal mesh extrusion rates between a lightweight type I polypropylene mesh versus heavier mesh in the treatment of pelvic organ prolapse. International urogynecology journal, 23 (2012) 1379–1386. doi: 10.1007/s00192-012-1744-9